Selected nucleon form factors and a composite scalar diquark

J. C. R. Bloch, C. D. Roberts, and S. M. Schmidt
Physics Division, Argonne National Laboratory, Argonne, Illinois 60439-4843
(Received 22 November 1999; published 22 May 2000)

A covariant, composite scalar diquark, Fadde'ev amplitude model for the nucleon is used to calculate pseudoscalar, isoscalar- and isovector-vector, axial-vector and scalar nucleon form factors. The last yields the nucleon σ term and on-shell σ-nucleon coupling. The calculated form factors are soft, and the couplings are generally in good agreement with experiment and other determinations. Elements in the dressed-quark-axial-vector vertex that are not constrained by the Ward-Takahashi identity contribute $\sim 20\%$ to the magnitude of g_A. The calculation of the nucleon σ term elucidates the only unambiguous means of extrapolating meson-nucleon couplings off the meson mass shell.

PACS number(s): 24.85.+p, 14.20.Dh, 13.75.Gx

I. INTRODUCTION

Current generation experiments probe hadrons and their interactions on a truly dynamical domain where symmetries alone are insufficient to characterize them. In this domain phenomenologically accurate nucleon-nucleon potentials [1,2] and meson exchange models [3] are keys in the interpretation of data. These models are tools via which the correlated quark exchange underlying hadron-hadron interactions is realized as a sum of the exchanges of elementary, mesonlike degrees of freedom,[1] and their definition relies on meson-nucleon form factors that sensibly provide short-range cutoffs in the integrals that arise in calculations.

These form factors are interpreted as a manifestation of the hadrons' internal structure. If this interpretation is realistic then they should be calculable in models that reliably describe hadron structure. This cannot mean that models of hadron structure should exactly reproduce the momentum dependence and parameter values used in potential models. In order to be phenomenologically successful, all models have hidden degrees of freedom, which make complicated a direct comparison between approaches. However, one can expect semiquantitative agreement, with large discrepancies being harbingers of model artefacts and defects.

An additional complication is that the mesons of the strong interaction spectrum are bound states and hence are only unambiguously defined on-shell; i.e., at their pole position in an n-point vertex function. Any reference to an off-shell meson is *necessarily* model dependent. Therefore, the only comparisons that can be model independent are those between calculated meson-baryon coupling constants and on-shell couplings inferred from potential models because these comparisons do not involve the *ad hoc* definition of an off-shell bound state.

Primarily for this reason, the comparison between calculated and phenomenological form factors can only be qualitative and should employ more than one off-shell extrapolation to provide reliable information. In spite of the ambiguities, however, the calculation of meson-baryon form factors is an essential element of contemporary phenomenology. For example, it can expose difficulties in phenomenological interpretations, as is well exemplified by the discussion of ρ^0-ω mixing and its contribution to charge symmetry breaking in NN potentials [4],[2] and also provide guidance in constraining meson exchange currents in light nuclear systems [6,7].

The dominant mesonlike degrees of freedom employed in potential models are identified with the π, ρ, ω and a light scalar, σ. Herein we calculate the associated meson-nucleon coupling constants and form factors using a covariant nucleon model [8]. It is motivated by quark-diquark solutions of a relativistic Fadde'ev equation [9–11] and while only retaining a scalar diquark correlation is a limitation, the model's treatment of that as a nonpointlike, confined composite is a significant beneficial feature. That is illustrated in its application to the calculation of nucleon electromagnetic form factors [8], which semiquantitatively describes the ratio $\mu_p G_E^p(q^2)/G_M^p(q^2)$ recently observed at TJNAF [12]. In Sec. II we review the model. Our results are described in the next four sections: Sec. III, πNN; Sec. IV, ωNN- and ρNN-like interactions; Sec. V explores the nucleon's axial-vector current; and Sec. VI focuses on the scalar-nucleon interaction. Section VII is a brief recapitulation and the Appendix contains selected formulas.

II. NUCLEON MODEL

We represent the nucleon as a three-quark bound state involving a nonpointlike diquark correlation and write its Fadde'ev amplitude as

[1]The extent to which these degrees of freedom are identified with the mesons of the strong interaction spectrum varies. In one-boson-exchange models [1] the identification is close, while in the Argonne series of potentials [2] the short-range part is interpreted as a purely phenomenological parametrization.

[2]It is an important and model-independent result that vector-channel resonant quark exchange is described by a vacuum polarization: $\Pi_{\mu\nu}(k)$, that vanishes at $k^2=0$ [5,6].

$$\Psi^{\tau}_{\alpha}(p_1,\alpha_1,\tau^1;p_2,\alpha_2,\tau^2;p_3,\alpha_3,\tau^3)$$
$$=\varepsilon_{c_1c_2c_3}\delta^{\tau\tau^3}\delta_{\alpha\alpha_3}\psi(p_1+p_2,p_3)$$
$$\times\Delta(p_1+p_2)\Gamma^{\tau^1\tau^2}_{\alpha_1\alpha_2}(p_1,p_2), \tag{1}$$

where $\varepsilon_{c_1c_2c_3}$ effects a singlet coupling of the quarks' color indices, (p_i,α_i,τ^j) denote the momentum and the Dirac and isospin indices for the ith quark constituent, α and τ are these indices for the nucleon itself, $\psi(l_1,l_2)$ is a Bethe-Salpeter-like amplitude characterizing the relative-momentum dependence of the correlation between diquark and quark, $\Delta(K)$ describes the propagation characteristics of the diquark, and

$$\Gamma^{\tau^1\tau^2}_{\alpha_1\alpha_2}(p_1,p_2)=(Ci\gamma_5)_{\alpha_1\alpha_2}(i\tau_2)^{\tau^1\tau^2}\Gamma(p_1,p_2) \tag{2}$$

represents the momentum dependence, and spin and isospin character of the diquark correlation; i.e., it corresponds to a Bethe-Salpeter-like amplitude for the diquark. While complete antisymmetrization is not explicit in Ψ, it is exhibited in our calculations via the exchange of roles between the dormant and diquark-participant quarks, and gives rise to diquark ''breakup'' contributions to the form factors. This is not an afterthought, it merely reflects the simple manner in which we choose to order and elucidate our calculations.

With the form of Ψ in Eq. (1), we retain in the quark-quark scattering matrix only the contribution of the scalar diquark, which has the largest correlation length [13]: $\lambda_{0^+}:=1/m_{0^+}=0.27$ fm. We saw as anticipated in Ref. [8] that the primary defect of Eq. (1) is the omission of the axial-vector correlation ($\lambda_{1^+}\approx 0.8\lambda_{0^+}$). Nevertheless, the *Ansatz* yielded much about the electromagnetic nucleon form factors that was quantitatively reliable and qualitatively informative. Hence, we employ it again herein as an exploratory, intuition building tool.

The amplitude in Eq. (1) is fully determined with the specification of the scalar functions:

$$\psi(l_1,l_2)=\frac{1}{\mathcal{N}_\Psi}\mathcal{F}(l^2/\omega_\psi^2),\quad l:=\tfrac{1}{3}l_1-\tfrac{2}{3}l_2, \tag{3}$$

$$\Gamma(q_1,q_2)=\frac{1}{\mathcal{N}_\Gamma}\mathcal{F}(q^2/\omega_\Gamma^2),\quad q:=\tfrac{1}{2}q_1-\tfrac{1}{2}q_2, \tag{4}$$

$$\Delta(K)=\frac{1}{m_\Delta^2}\mathcal{F}(K^2/\omega_\Gamma^2), \tag{5}$$

$$\mathcal{F}(y)=\frac{1-e^{-y}}{y}, \tag{6}$$

which introduces three parameters whose values were determined [8] in a least-squares fit to $G_E^p(q^2)$:

ω_ψ	ω_Γ	m_Δ
0.20	1.4	0.63

(7)

all in GeV ($1/m_\Delta=0.31$ fm).[3] $\mathcal{N}_\Psi$ and $\mathcal{N}_\Gamma$ are the *calculated* nucleon and (ud) diquark normalization constants, which via the canonical definition ensure composite electric charges of 1 for the proton and 1/3 for the diquark. Current conservation is manifest in this model.

An essential, additional element in the calculation of the electromagnetic nucleon form factors is the dressed-quark propagator:

$$S(p)=-i\gamma\cdot p\sigma_V(p^2)+\sigma_S(p^2) \tag{8}$$
$$=[i\gamma\cdot pA(p^2)+B(p^2)]^{-1}. \tag{9}$$

While $S(p)$ can be obtained as a solution of the quark Dyson-Schwinger equation (DSE) [14], a phenomenologically efficacious algebraic parametrization has been determined in extensive studies of meson properties [15,16] and we employ it herein:

$$\bar{\sigma}_S(x)=2\bar{m}\mathcal{F}(2(x+\bar{m}^2))+\mathcal{F}(b_1x)\mathcal{F}(b_3x)[b_0+b_2\mathcal{F}(\epsilon x)], \tag{10}$$

$$\bar{\sigma}_V(x)=\frac{1}{x+\bar{m}^2}[1-\mathcal{F}(2(x+\bar{m}^2))], \tag{11}$$

$x=p^2/\lambda^2$, $\bar{m}=m/\lambda$, $\bar{\sigma}_S(x)=\lambda\sigma_S(p^2)$, and $\bar{\sigma}_V(x)=\lambda^2\sigma_V(p^2)$. The mass scale, $\lambda=0.566$ GeV, and parameter values

$\bar{m}$	b_0	b_1	b_2	b_3
0.00897	0.131	2.90	0.603	0.185

(12)

were fixed in a least-squares fit to light-meson observables [15]. [$\epsilon=10^{-4}$ in Eq. (10) acts only to decouple the large- and intermediate-p^2 domains.] This algebraic parametrization combines the effects of confinement and dynamical chiral symmetry breaking with free-particle behavior at large spacelike p^2 [16].

III. PION NUCLEON COUPLING

The pion-nucleon current is

$$J^j_\pi(P',P)=\bar{u}(P')\Lambda^j_\pi(q,P)u(P) \tag{13}$$
$$=:g_{\pi NN}(q^2)\bar{u}(P')i\tau^j\gamma_5u(P), \tag{14}$$

where the spinors satisfy

$$\gamma\cdot Pu(P)=iMu(P),\quad \bar{u}(P)\gamma\cdot P=iM\bar{u}(P) \tag{15}$$

with the nucleon mass $M=0.94$ GeV and $q=(P'-P)$.

[3]This modified value of ω_Γ arises from correcting a minor computational error in the calculations of Ref. [8]. In our Euclidean formulation: $p\cdot q=\Sigma_{i=1}^4p_iq_i$, $\{\gamma_\mu,\gamma_\nu\}=2\delta_{\mu\nu}$, $\gamma_\mu^\dagger=\gamma_\mu$, $\sigma_{\mu\nu}=i/2\,[\gamma_\mu,\gamma_\nu]$, and $\mathrm{tr}_D[\gamma_5\gamma_\mu\gamma_\nu\gamma_\rho\gamma_\sigma]=-4\epsilon_{\mu\nu\rho\sigma}$, $\epsilon_{1234}=1$.

For an on-shell pion a calculation of the impulse approximation to J^j_π requires only one additional element: $\Gamma^j_\pi(k;Q)$, the pion Bethe-Salpeter amplitude, with k being the relative quark-antiquark momentum and Q is the total momentum of the bound state. It has the general form

$$\Gamma^j_\pi(k;Q)=\tau^j\gamma_5[iE_\pi(k;Q)+\gamma\cdot QF_\pi(k;Q) + \gamma\cdot k k\cdot Q G_\pi(k;Q)+\sigma_{\mu\nu}k_\mu Q_\nu H_\pi(k;Q)], \tag{16}$$

and is obtained as a solution of a homogeneous Bethe-Salpeter equation.

Using any truncation of the quark-antiquark scattering matrix that ensures the preservation of the axial-vector Ward-Takahashi identity then, in the chiral limit [17],

$$E_\pi(k;Q=0)=\frac{1}{f_\pi}B_0(k^2), \tag{17}$$

and F_π, G_π, H_π satisfy similar relations involving $A_0(k^2)$. Here f_π is the pion decay constant and $A_0(k^2)$, $B_0(k^2)$ are the dressed-quark propagator functions in Eq. (9) calculated in the chiral limit. Since [14,16]

$$A(p^2)\neq 1, \tag{18}$$

the identities involving F_π, G_π, H_π entail that the pion necessarily has pseudovector components, even in the chiral limit. These components are crucial at large pion energy; e.g., they are responsible for the asymptotic $1/q^2$ behavior of the electromagnetic pion form factor [18], however, for pion energy $\lesssim 1$ GeV they are quantitatively unimportant, and Eq. (16) with Eq. (17) and $F_\pi=0=G_\pi=H_\pi$ provides a reliable approximation.

This fact is useful in phenomenological applications, and away from the chiral limit an algebraic parametrization has been developed [15,19] to be used in concert with Eqs. (10),(11):

$$E_\pi(k;Q)=\frac{1}{f_\pi}B_\pi(k^2), \tag{19}$$

where $B_\pi(k^2)$ is obtained from Eqs. (9)–(11) with [20]

$$\overline{m}\to 0,\quad b_0\to b_0^\pi=0.204. \tag{20}$$

This form of dressed-quark propagator and pion Bethe-Salpeter amplitude yields (quoted with GeV as the base unit)

	f_π	m_π	$\langle\overline{q}q\rangle_0^{1\ \mathrm{GeV}^2}$	$\langle\overline{q}q\rangle_\pi^{1\ \mathrm{GeV}^2}$
Calc.	0.0924	0.141	$(0.221)^3$	$(0.257)^3$
Obs. [21,22]	0.0924	0.138	$(0.241)^3$	$(0.245)^3$

(21)

where $\langle\overline{q}q\rangle_0^{1\ \mathrm{GeV}^2}$ is the vacuum quark condensate and $\langle\overline{q}q\rangle_\pi^{1\ \mathrm{GeV}^2}$ is the ''in-pion'' condensate, which appears in the pseudoscalar meson mass formula derived in Ref. [17] and further elucidated in Refs. [20,22].

The (on-shell) Bethe-Salpeter amplitude is sufficient to calculate the pion-nucleon coupling. However, to calculate the form factor we must specify an off-shell extrapolation of $E_\pi(k;Q)$; i.e., a functional dependence for $Q^2\neq -m_\pi^2$. Two obvious *Ansätze* are

$$\text{(a)}\quad f_\pi\tilde{E}_\pi(k;Q)=B_\pi(k^2), \tag{22}$$

$$\text{(b)}\quad f_\pi\tilde{E}_\pi(k;Q)=\frac{1}{2}[B_\pi(k_+^2)+B_\pi(k_-^2)], \tag{23}$$

with $k_\pm=k\pm Q/2$. The first, which assumes no change off shell, has been used with phenomenological success in a variety of calculations that explore meson-loop corrections to hadronic observables [23]; the second [14] allows some minimal dependence on $k\cdot Q$, Q^2; and for $Q=0$ both satisfy the constraint of Eq. (19) [cf. Eq. (17)].

As with the electromagnetic form factors, five distinct diagrams contribute to the nucleon form factors, which are depicted in Fig. 1. For the πNN coupling these diagrams, enumerated from top to bottom, are mnemonics for the vertices $\Lambda^{nj}_\pi(q,P)$ given in Eqs. (A1)–(A5). As can be anticipated, $\Lambda^{2j}_\pi(q,P)\equiv 0$ because of parity conservation; i.e., a Poincaré invariant theory cannot admit a three-point pseudoscalar-scalar-scalar coupling.

The pion-nucleon vertex:

$$\Lambda^j_\pi(q,P)=\Lambda^{1j}_\pi(q,P)+2\sum_{n=2}^{5}\Lambda^{nj}_\pi(q,P), \tag{24}$$

is completely expressed in terms of four independent scalar functions

$$\Lambda^j_\pi(q,P)=\tau^j\gamma_5[if_1+\gamma\cdot q f_2+\gamma\cdot R f_3+\sigma_{\mu\nu}R_\mu q_\nu f_4], \tag{25}$$

where $f_i=f_i(q^2)$, $R=(P'+P)$ and $q\cdot R=0$ for nucleon elastic scattering. From this we construct the pion-nucleon current

$$J^j_\pi(P',P)=\overline{u}(P')\Lambda^j_\pi(q,P)u(P), \tag{26}$$

and employing the definition of the nucleon spinors, Eqs. (15), we identify the pion-nucleon coupling in Eq. (13):

$$g_{\pi NN}(q^2)=f_1-2Mf_2+R^2f_4. \tag{27}$$

Using Monte Carlo methods to evaluate the integrals we obtain the coupling, $g_{\pi NN}:=g_{\pi NN}(q^2=0)$, in Table I. It is 11% too large. (Our statistical error is always $<1\%$.) We anticipate that retaining pseudovector components in $\Gamma^j_\pi(k;Q)$ and an axial-vector diquark correlation will only slightly affect this value as long as they are constrained *consistently* with the model. An *ad hoc* addition of the pseudovector components can have large effects [26].

The relative strength of the contribution from each diagram in Fig. 1 is presented in Table II. We observe that the diquark breakup terms are just as important here as they were in the calculation of the nucleon charge radii and magnetic moments [8]. These diagrams are the true measure of the

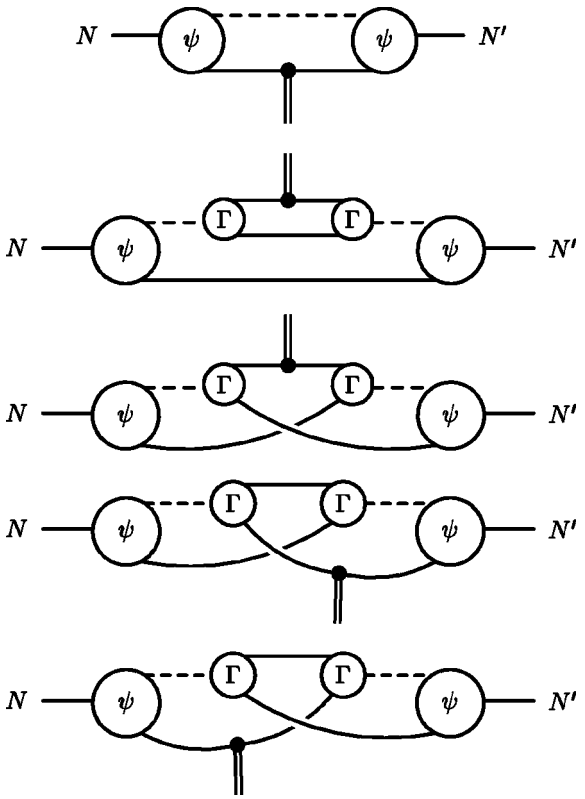

FIG. 1. Our impulse approximation to the meson-nucleon form factors requires the calculation of five contributions, which differ in detail for each probe. ψ: $\psi(l_1,l_2)$ in Eq. (3); Γ: Bethe-Salpeter-like diquark amplitude in Eq. (2); dashed line: $\Delta(K)$, diquark propagator in Eq. (5); solid internal line: $S(q)$, quark propagator in Eq. (8); and double line: mesonlike probe. The lowest three diagrams, which describe the interchange between the dormant quark and the diquark participants, effect the antisymmetrization of the nucleon's Fadde'ev amplitude.

diquark's composite nature, which is not captured by simply adding a diquark ''vertex function.''

The πNN form factor calculated using both off-shell *Ansätze*, Eqs. (22),(23), is plotted in Fig. 2. We have performed monopole and dipole fits to our calculated result:

$$g_{\pi NN}(q^2)=\frac{g_{\pi NN}}{(1+q^2/\Lambda_\pi^2)^n}, \quad n=1,2, \tag{28}$$

and obtain pole masses, in GeV,

	$n=1$	$n=2$
Eq. (22)	0.63	0.96
Eq. (23)	0.57	0.85.

(29)

The dipole form provides an accurate interpolation on the entire range shown. However, the monopole form is only accurate for $q^2 \lesssim 0.4$ GeV^2, overestimating the result by $\sim 70\,\%$ at $q^2=3.0$ GeV^2. (Requiring that the fits are accurate in the neighborhood of $q^2=0$ ensures $\Lambda_\pi^{\rm dipole}/\Lambda_\pi^{\rm monopole} \approx \sqrt{2}$.) Thus our calculations favor soft form factors, in semi-quantitative agreement with those employed in Ref. [3] and advocated in Ref. [27]. We can further quantify this by introducing a pionic radius of the nucleon:

$$\langle r^2_{\pi NN}\rangle := -\frac{6}{g_{\pi NN}}\frac{dg_{\pi NN}(q^2)}{dq^2}\bigg|_{q^2=0}. \tag{30}$$

Our calculated value is presented in Table I and can be compared with the analogous tabulated quantities. It is almost three times larger than $r_{\pi NN}\sim 0.3$ fm inferred from Ref. [1].

TABLE I. Calculated couplings compared with: contemporary meson exchange model values [3], where available; experiment in the case of g_A, r_A [24]; a lattice-QCD result for σ [25]; and for g_σ, r_σ, as discussed in connection with Eqs. (84)–(87). Also for comparison, the pion model described in Sec. II yields [15] $r_\pi=0.56$ fm. The labels (a) etc. identify the results obtained with Eqs. (22),(23) for πNN; Eqs. (38),(39),(41) for VNN; and Eqs. (60),(61) for the axial-vector coupling.

	Calc.	Estimates	Expt.
$g_{\pi NN}$	14.9	13.4	
$\langle r^2_{\pi NN}\rangle^{1/2}$	(a) 0.71 (b) 0.80	0.93–1.06 fm	
$g_{\rho NN}$	(a) 5.92 (b) 6.26 (c) 4.82	6.4	
$f_{\rho NN}$	(a) 15.4 (b) 16.6 (c) 12.6	13.0	
κ_ρ	(a) 2.57 (b) 2.64 (c) 2.61	2.0	
$g_{\omega NN}$	(a) 9.74 (b) 10.2 (c)11.5	7–10.5	
$f_{\omega NN}$	(a) 9.62 (b) 10.7 (c) 4.39		
κ_ω	(a) 0.99 (b) 1.04 (c) 0.38		
g_A	(a) 0.80 (b) 0.99		1.259 ± 0.017
$\langle r^2_A\rangle^{1/2}$	(a) 0.75 (b) 0.75		0.68 ± 0.12 fm
σ/M_N	0.015	0.019 ± 0.05	
g_σ	9.3	10	
$\langle r^2_{\sigma NN}\rangle^{1/2}$	0.89	1.2 fm	

IV. VECTOR-MESON NUCLEON COUPLING

In this section we consider ω-NN- and ρ-NN-like interactions; i.e., isoscalar-vector and isovector-vector couplings. The vector-meson–nucleon current is

TABLE II. Relative contribution to the couplings of each of the terms represented mnemonically by the five diagrams in Fig. 1. In building this table we used the amplitudes in Eq. (22) for the π, Eqs. (38),(41) for the vector couplings, and the dressed-quark-axial-vector vertex of Eqs. (57),(61). In all cases the crucial role of the diquark breakup diagrams is evident. Diagram 2 will contribute to all processes if an axial-vector diquark correlation is included.

	Diagram	1	2	3	4	5
$g_{\pi NN}$		0.65	0.00	0.07	0.14	0.14
$g_{\rho NN}$	(a)	0.74	0.00	−0.06	0.16	0.16
	(c)	0.73	0.00	−0.11	0.19	0.19
$f_{\rho NN}$	(a)	0.64	0.00	0.10	0.13	0.13
	(c)	0.64	0.00	0.12	0.12	0.12
$g_{\omega NN}$	(a)	0.45	0.31	0.04	0.10	0.10
	(c)	0.31	0.49	0.05	0.08	0.08
$f_{\omega NN}$	(a)	1.04	−0.28	−0.16	0.20	0.20
	(c)	1.81	−1.16	−0.35	0.35	0.35
g_A		0.63	0.00	0.09	0.14	0.14
σ		0.58	0.19	0.03	0.10	0.10

$$J_\mu^{V\alpha}(P',P)=i\overline{u}(P')\frac{\tau^\alpha}{2}\Big(\gamma_\mu F_1^V(q^2)+\frac{1}{2M}\sigma_{\mu\nu}q_\nu F_2^V(q^2)\Big)u(P), \tag{31}$$

with $\tau^0:=\mathrm{diag}(1,1)$ and $\tau^{1,2,3}$ the usual Pauli matrices. Although the complete specification of a fermion-vector boson vertex,

$$\Lambda_\mu^\alpha(q,P):=\frac{\tau^\alpha}{2}\Lambda_\mu(q,P), \tag{32}$$

requires 12 independent scalar functions,

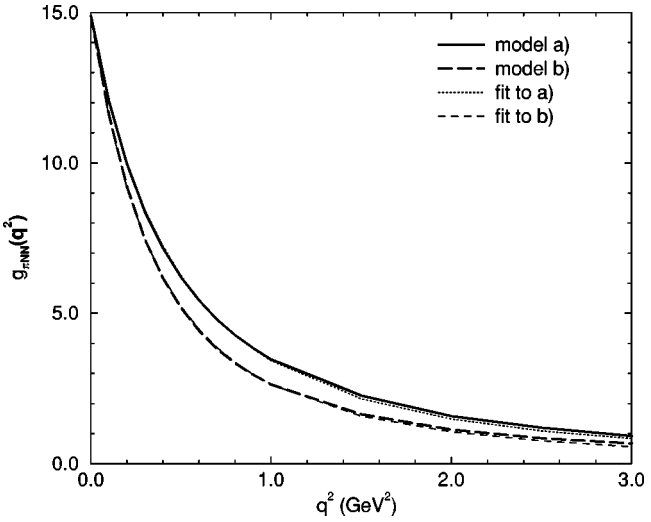

FIG. 2. Calculated pion-nucleon form factor, compared with dipole fits, Eqs. (28),(29).

$$i\Lambda_\mu(q,P)=i\gamma_\mu f_1+i\sigma_{\mu\nu}q_\nu f_2+R_\mu f_3+i\gamma\cdot R R_\mu f_4+i\sigma_{\nu\rho}R_\mu q_\nu R_\rho f_5+i\gamma_5\gamma_\nu\varepsilon_{\mu\nu\rho\sigma}q_\rho R_\sigma f_6+\cdots, \tag{33}$$

using Eq. (15) only the six shown explicitly contribute to $F_{1,2}$:

$$F_1=f_1+2Mf_3-4M^2f_4-2Mq^2f_5-q^2f_6, \tag{34}$$

$$F_2=2Mf_2-2Mf_3+4M^2f_4+2Mq^2f_5-4M^2f_6. \tag{35}$$

The coupling strengths relevant for comparison with potential models are

$$g_{VNN}:=F_1^V(0),\quad f_{VNN}:=F_2^V(0),\quad \kappa_V:=\frac{f_{VNN}}{g_{VNN}} \tag{36}$$

because these are t-channel elastic-scattering models. However, we note that $q^2=0$ is a far off-shell point for the ω and ρ of the strong interaction spectrum, for which $(-q^2)=M_V^2\approx 0.6$ GeV^2. Hence a calculation of these coupling constants is only possible after an off-shell extrapolation of the vector meson Bethe-Salpeter amplitude is specified.

Quantitatively reliable numerical solutions of the vector meson Bethe-Salpeter equation have recently become available [28], however, an algebraic *Ansatz* compatible with our parametrization of the dressed-quark propagator, Eqs. (10),(11), is not yet available. Hence, we use *Ansätze* motivated by an extensive study of light- and heavy-meson observables [20]:

$$\Gamma_\mu^\alpha(k;Q)=\frac{1}{\mathcal{N}_V}\Big(\gamma_\mu-\frac{Q_\mu\gamma\cdot Q}{Q^2}\Big)\varphi(k^2)\tau^\alpha, \tag{37}$$

$$\text{(a)}\quad \varphi(k^2)=1/(1+k^4/\omega^4), \tag{38}$$

$$\text{(b)}\quad \varphi(k^2)=[\mathcal{F}(k^2/\omega^2)]^2, \tag{39}$$

with $\omega=0.515$ GeV and the normalization: $\mathcal{N}_V$, determined canonically, Eq. (A12). Following Ref. [20], using these simple forms of $\Gamma_\mu^\alpha(k;Q)$ in the appropriate formulas therein, we calculate values of the electromagnetic and strong coupling constants, columns (a), (b):

	Obs. [21]	(a)	(b)	(c)
g_ρ	5.03±0.012	6.57	6.05	4.37
$g_{\rho\pi\pi}$	6.05±0.02	8.75	10.7	8.52.

(40)

These results suggest that errors of up to 40% could arise in nucleon calculations involving these amplitudes.

The calculation of the vector-meson–nucleon current is now straightforward with $F_{1,2}$ determined by calculating the integrals in Eqs. (A7)–(A11) and combining their contributions according to Eqs. (34),(35),(A13). In this way we obtain the couplings presented in Table I, with the relative strength of the contribution from each diagram given in Table II.

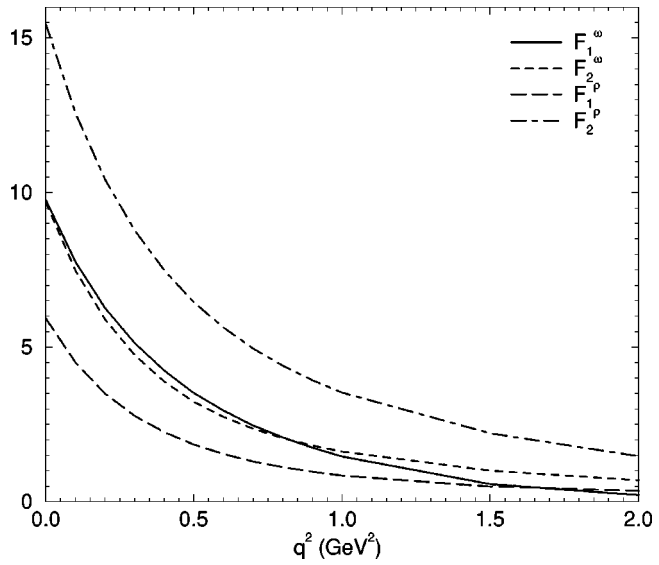

FIG. 3. Calculated vector-meson–nucleon form factors. A good interpolation of the results is obtained with Eqs. (43),(44).

The couplings are in semiquantitative agreement with those inferred from meson-exchange models [3] *except* in the case of $f_{\omega NN}$. Using Eqs. (38),(39) we obtain $f_{\omega NN} \approx g_{\omega NN}$ while contemporary phenomenological models, which are only weakly sensitive to $f_{\omega NN}$, assume it to be zero. To determine the extent to which this result is model dependent, we also calculate the couplings using

$$\text{(c)} \quad \varphi(k^2) = \frac{1}{\mathcal{N}_V} B_V(k^2), \tag{41}$$

where $B_V(k^2)$ is obtained from Eqs. (9)–(11) with [19] $\overline{m} \to 0$ and

$$b_0 \to b_0^V = 0.044, \quad b_1 \to b_1^V = 0.580, \quad b_3 \to b_3^V = 0.462. \tag{42}$$

The amplitude is canonically normalized via Eq. (A12) and Ref. [19] reports the values of g_ρ, $g_{\rho\pi\pi}$ in column *c*) of Eq. (40).

The nucleon couplings are given in Table I with the relative strength of the contribution from each diagram presented in Table II. In this case, while the other couplings change by $\lesssim 20\,\%$, we find $f_{\omega^{c)}NN} \approx 0.4\, g_{\omega^{c)}NN}$. The reason appears in Table II: the strength of diagram 2 is much increased, and while it does not contribute at all for the ρ and is additive for $g_{\omega NN}$, it is a destructive contribution to $f_{\omega NN}$. This sensitivity to cancellations involving diagram 2 repeats the pattern we observed in calculating the nucleon's isoscalar electromagnetic form factor [8] and hence $f_{\omega NN}$ is sensitive to the omission of the axial-vector diquark correlation.

The vector-meson–nucleon form factors calculated using Eq. (38) are depicted in Fig. 3 and the quadrupole

$$F_n^V(q^2) = F_n^V(0) \frac{1}{(1 + q^2/\Lambda_n^V)^3} \tag{43}$$

with pole masses, in GeV,

$$\begin{array}{cccc} \Lambda_1^\omega & \Lambda_2^\omega & \Lambda_1^\rho & \Lambda_2^\rho \\ 1.12 & 1.11 & 1.06 & 1.18 \end{array} \tag{44}$$

provides an excellent interpolation of the results. Again, these are soft form factors.

On the domain explored, our results for the *VNN* form factor are qualitatively unaffected by employing a monopole for $\varphi(k^2)$ in Eq. (37).

V. AXIAL-VECTOR NUCLEON COUPLING

Neutron β decay is described by the axial-vector–nucleon current

$$J_{5\mu}^j(P',P) = i\overline{u}(P')\Lambda_{5\mu}^j(q,P)u(P) \tag{45}$$

$$=: i\overline{u}(P')\gamma_5 \frac{\tau^j}{2}[\gamma_\mu g_A(q^2) + q_\mu g_P(q^2)]u(P), \tag{46}$$

which involves two form factors: $g_A(q^2)$ is the axial-vector form factor of the nucleon and $g_P(q^2)$ is the induced pseudoscalar form factor. The complete specification of a fermion-axial-vector vertex,

$$\Lambda_{5\mu}^j(q,P) =: \frac{\tau^j}{2}\Lambda_{5\mu}(q,P), \tag{47}$$

requires 12 independent scalar functions,

$$\Lambda_{5\mu}(q,P) = \gamma_5\gamma_\mu f_1 + \gamma_5\sigma_{\mu\nu}R_\nu f_2 + \epsilon_{\mu\nu\rho\sigma}\gamma_\nu q_\rho R_\sigma f_3 + \cdots \tag{48}$$

but using Eqs. (15) only the three shown explicitly contribute to the axial-vector form factor

$$g_A(q^2) = f_1 - 2Mf_2 - q^2 f_3. \tag{49}$$

In the chiral limit and in the neighborhood of $q^2 = 0$ [17,22]

$$\Lambda_{5\mu}^j(q,P) = \text{regular} + \frac{q_\mu}{q^2} f_\pi \Lambda_\pi^j(q,P), \tag{50}$$

where $\Lambda_\pi^j(q,P)$ is the pion-fermion vertex and *regular* denotes nonpole terms. It follows that in this neighborhood the induced pseudoscalar coupling is dominant and, using Eq. (13), is determined by the pion-nucleon coupling:

$$q^2 J_{5\mu}^j(P',P)|_{q^2=0} = q_\mu f_\pi g_{\pi NN}(q^2=0)\overline{u}(P')i\tau^j\gamma_5 u(P) \tag{51}$$

$$= q_\mu \overline{u}(P')\gamma_5 \frac{\tau^j}{2}[q^2 g_P(q^2)]_{q^2=0} u(P). \tag{52}$$

Current conservation: $q_\mu J_{5\mu}^j(q,P) = 0$, which using Eqs. (15) entails

$$-2Mg_A(q^2=0)+[q^2g_P(q^2)]|_{q^2=0}=0, \tag{53}$$

then yields the Goldberger-Treiman relation:

$$Mg_A(q^2=0)=f_\pi g_{\pi NN}(q^2=0). \tag{54}$$

This brief analysis emphasizes that $g_A(q^2)$ is the *regular* part of the axial-vector–nucleon current.

To calculate $g_A(q^2)$ in the impulse approximation we must specify the dressed-quark-axial-vector vertex: $\Gamma^j_{5\mu}(k;Q)$. It satisfies a Ward-Takahashi identity, which in the chiral limit is

$$-iQ_\mu\Gamma^j_{5\mu}(k;Q)=S^{-1}(k_+)\gamma_5\frac{\tau^j}{2}+\gamma_5\frac{\tau^j}{2}S^{-1}(k_-). \tag{55}$$

This identity is solved by

$$\Gamma^j_{5\mu}(k;Q)=\Gamma^{Rj}_{5\mu}(k;Q)+\gamma_5\frac{\tau^j}{2}\left[i\frac{Q_\mu}{Q^2}2\Sigma_B(k_+^2,k_-^2)\right], \tag{56}$$

$$\Gamma^{Rj}_{5\mu}(k;Q)=\Gamma^{Tj}_{5\mu}(k;Q)+\gamma_5\frac{\tau^j}{2}(\gamma_\mu\Sigma_A(k_+^2,k_-^2) +2k_\mu\gamma\cdot k\Delta_A(k_+^2,k_-^2)), \tag{57}$$

where $Q_\mu\Gamma^{Tj}_{5\mu}(k;Q)=0$ but $\Gamma^{Tj}_{5\mu}(k;Q)$ is otherwise unconstrained by the Ward-Takahashi identity and

$$\Sigma_f(p^2,q^2):=\tfrac{1}{2}[f(p^2)+f(q^2)], \tag{58}$$

$$\Delta_f(p^2,q^2):=\frac{f(p^2)-f(q^2)}{p^2-q^2}. \tag{59}$$

The parenthesized term in Eq. (56) makes explicit the simple kinematic singularity associated with the pion pole.[4] It is directly connected with the nucleon's induced pseudoscalar form factor and, using Eqs. (17),(23), clearly saturates Eq. (51). The regular part of the vertex, Eq. (57), is primarily responsible for the nucleon's axial-vector form factor and in our calculations we complete its definition using either of two *Ansätze* for the transverse part:

$$\text{(a)}\quad \Gamma^{Tj}_{5\mu}(k;Q)=0, \tag{60}$$

$$\text{(b)}\quad \Gamma^{Tj}_{5\mu}(k;Q)=\frac{1}{\sqrt{2}}\frac{f_{a_1}m_{a_1}}{Q^2+m^2_{a_1}}\Gamma^{a_1j}_\mu(k;Q), \tag{61}$$

where $\Gamma^{a_1j}_\mu(k;Q)$ is the a_1-meson Bethe-Salpeter amplitude, which is given explicitly in Eq. (A14). Model (a): Eqs. (57),(60), is a minimal *Ansatz* that correctly isolates the pion pole. Model (b): Eqs. (57),(61), is kindred to that advocated for the dressed-quark-vector vertex in Ref. [29]. It recognizes that the dressed-quark-axial-vector vertex has a pole at $Q^2=-m^2_{a_1}$ with residue $f_{a_1}m_{a_1}$ where f_{a_1} is the weak decay constant, and implements a model to represent the off-shell remnant of this contribution.

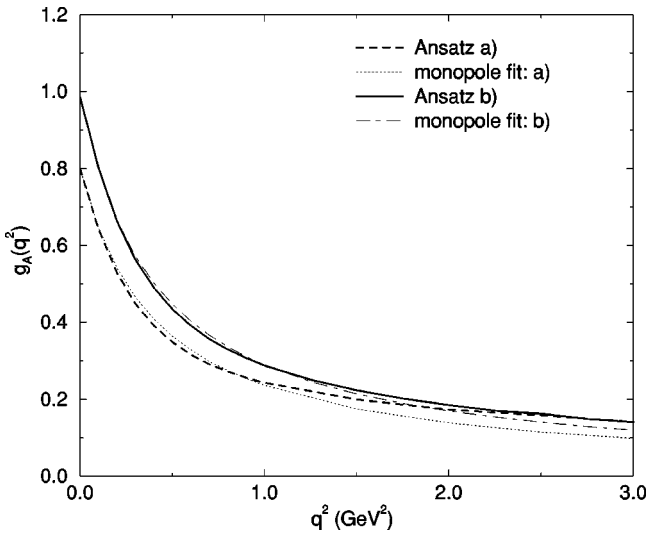

FIG. 4. Axial-vector–nucleon form factor calculated using the *Ansätze* of Eqs. (60),(61) compared with a monopole fit, Eqs. (62),(63).

$g_A(q^2)$ is obtained by evaluating the integrals in Eqs. (A22)–(A26) and combining their contributions according to Eqs. (49),(A27). The calculated coupling is presented in Table I with the relative strength of the contribution from each diagram given in Table II.[5]

The axial-vector form factor is depicted in Fig. 4. It is important and interesting to note that the dominant, orbital $e_2^{a_1}$ term in $\Gamma^{a_1}_\mu$ [see Eqs. (A14)–(A21)] contributes $<10\%$ to $g_A(q^2)$ on the illustrated domain, increasing from 0% with increasing q^2; i.e., the bulk of the difference between the (a) and (b) calculations arises from the $e_1^{a_1}$ term. In Fig. 4 we also plot a monopole fit to each calculation

$$g_A(q^2)=g_A(0)\frac{1}{(1+q^2/\Lambda_A^2)} \tag{62}$$

with pole masses, in GeV,

	(a)	(b)
Λ_A	0.65	0.64

(63)

[4]Using $(k_\mu/k\cdot Q)\Sigma_B(k_+^2,k_-^2)$ in Eq. (56) instead of the parenthesized term is inadequate in this respect. Further, to exacerbate this flaw, it also introduces nonintegrable singularities in diagrams (3)–(5).

[5]We are unable to reproduce the large value of g_A obtained in Ref. [32]. Some of the discrepancy may be due to our simplified representation of the quark+scalar-diquark nucleon spinor in Eq. (1) [33]. However, that does not diminish the importance of $\Gamma^{Tj}_{5\mu}$.

The fit provides a better representation for *Ansatz* (b) than for (a), and we judge (b) to be the more realistic model. The axial radius of the nucleon is

$$\langle r_A^2\rangle := -\frac{6}{g_A(0)}\frac{dg_A(q^2)}{dq^2}\bigg|_{q^2=0} \tag{64}$$

and our calculated value is presented in Table I: $r_A \approx r_{\pi NN}$ in accordance with Ref. [27].

Even though our framework manifestly preserves the axial-vector Ward-Takahashi identity the model is not guaranteed to satisfy the Goldberger-Treiman relation because we employ *Ansätze* for the Fadde'ev amplitude and the dressed-quark-axial-vector vertex that need not be mutually consistent. For example, in deriving Eq. (54) we used Eqs. (15), which introduce M, however, Ψ in Eq. (1) is not the solution of a Fadde'ev equation with eigenvalue M. Indeed, without an axial-vector diquark correlation, the calculated nucleon mass is 30–50 % too large [10,34,35]. The following comparisons (in GeV) exhibit this uncertainty:

$$\left.\begin{array}{ll}\text{(a)} & Mg_A(0)=0.75-1.1\\ \text{(b)} & Mg_A(0)=0.93-1.4\end{array}\right\} \quad \text{cf. } f_\pi g_{\pi NN}=1.37, \tag{65}$$

and show that model *Ansatz* (b) is broadly consistent with the Goldberger-Treiman relation.

A comparison between the results obtained with the two-vertex *Ansätze* demonstrates that a calculation of the dressed-quark-axial-vector vertex, akin to that of the dressed-quark-vector vertex in Ref. [29], would be very helpful in demarcating the importance of axial-vector diquark correlations. As shown by the model (b) calculation, $\Gamma^{Tj}_{5\mu}$ easily provides contributions of the same order of magnitude as that which might be anticipated from an axial-vector diquark.

VI. NUCLEON σ TERM

As a final application we explore the nucleon σ term:

$$\sigma(q^2)\overline{u}(P')u(P) := \langle P'|m(\overline{u}u+\overline{d}d)|P\rangle, \tag{66}$$

$\sigma := \sigma(q^2=0)$, which is the in-nucleon expectation value of the explicit chiral symmetry breaking term in the QCD Lagrangian. The general form for a fermion-scalar vertex is

$$\Lambda_{\mathbf{1}}(q,P) = f_1 + i\gamma\cdot q f_2 + i\gamma\cdot R f_3 + i\sigma_{\mu\nu}R_\mu q_\nu f_4, \tag{67}$$

however, using Eqs. (15) we find

$$J_{\mathbf{1}}(P',P) := \overline{u}(P')\Lambda_{\mathbf{1}}(q,P)u(P) \tag{68}$$

$$= s(q^2)\overline{u}(P')u(P), \tag{69}$$

$$s(q^2) = f_1 - 2Mf_3 + q^2 f_4. \tag{70}$$

To evaluate the matrix element in Eq. (66) we need the dressed-quark-scalar vertex, which is an analog of the dressed-quark-axial-vector vertex used in Sec. V. In this case, however, there is not a Ward-Takahashi identity to help us. Instead, we calculate the vertex by solving an inhomogeneous Bethe-Salpeter equation using a simple, separable model for the quark-antiquark scattering kernel [13] that has been used successfully in a variety of phenomenological applications [30,36].

The inhomogeneous vertex equation in the separable model is

$$\Gamma_{\mathbf{1}}(k;Q) = \mathbf{1} - \tfrac{4}{3}\int\frac{d^4q}{(2\pi)^4}\Delta(k-q)\gamma_\mu S(q_+) \times\Gamma_{\mathbf{1}}(q;Q)S(q_-)\gamma_\mu, \tag{71}$$

with the interaction

$$\Delta(k-q) = G(k^2)G(q^2) + k\cdot q F(k^2)F(q^2), \tag{72}$$

where

$$F(k^2) = \frac{1}{a}[A(k^2)-1], \quad G(k^2) = \frac{1}{b}[B(k^2)-\tilde{m}], \tag{73}$$

$a = \overline{a}\lambda^2$, $b = \overline{b}\lambda^2$, and $A(k^2)$, $B(k^2)$ are obtained in the usual way from Eqs. (A17),(A18) with $\tilde{m} = \hat{m}\lambda$ and $b_2^{a_1} \to b_2$. The separable model was constrained to fit π and K properties, as discussed in detail in Ref. [13].

Using this model the most general form of the scalar vertex is

$$\Gamma_{\mathbf{1}}(k;Q) = \mathbf{1}g_1 + ik\cdot Q\gamma\cdot Q g_2 + i\gamma\cdot k g_3, \tag{74}$$

where $g_i = g_i(k;Q)$. Substituting Eq. (74) in Eq. (71) we obtain the solution

$$\Gamma_{\mathbf{1}}(k;Q) = \mathbf{1} + t_1(Q^2)G(k^2) + it_2(Q^2)F(k^2)\frac{k\cdot Q\gamma\cdot Q}{Q^2} + it_3(Q^2)F(k^2)\gamma\cdot k, \tag{75}$$

where $t_{1,2,3}(Q^2)$ are calculated functions of their argument; i.e., of Q^2 only.

The σ term is only sensitive to the vertex at $Q^2=0$, where the explicit form of the solution reduces to

$$\Gamma_{\mathbf{1}}(k;Q)|_{Q^2=0} = \mathbf{1} + t_1(0)G(k^2) + t_3(0)F(k^2)i\gamma\cdot k, \tag{76}$$

with $t_1(0)=0.242$ GeV, $t_3(0)=-0.0140$ GeV. It is important to note from Eqs. (73),(76) that the t_1 term contributes $1.4\times[B(k^2)-\tilde{m}]/\sqrt{b}$ so that at $k^2=0$ it is six times larger than the bare term; i.e., it is dominant in the infrared. That is to be expected because it represents the effect of the nonperturbative dynamical chiral symmetry-breaking mechanism in the solution. This and the other t_i terms vanish as $k^2\to\infty$, which is a manifestation of asymptotic freedom in the separable model.

The vertex equation has a solution for all Q^2, and that solution exhibits a pole at the σ-meson mass; i.e., in the neighborhood of $(-Q^2) = m_\sigma^2 = (0.715\ \text{GeV})^2$

$$\Gamma_{\mathbf{1}}(k;Q) = regular + \frac{n_\sigma m_\sigma^2}{Q^2 + m_\sigma^2}\Gamma_\sigma(k;Q), \tag{77}$$

where *regular* indicates terms that are regular in this neighborhood and $\Gamma_\sigma(k;Q)$ is the canonically normalized σ-meson Bethe-Salpeter amplitude, whose form is exactly that of $[\Gamma_{\mathbf{1}}(k;Q) - \mathbf{1}]$ in Eq. (75). The simple pole appears in the functions $t_i(Q^2)$ and performing a pole fit we find

$$m n_\sigma = 3.3 \ \text{MeV}. \tag{78}$$

$n_\sigma m_\sigma^2$ is the analog of the residue of the pion pole in the pseudoscalar vertex [17,22]: $-\langle \bar{q}q \rangle_\pi / f_\pi$, and its flow under the renormalization group is identical. $m n_\sigma$ is renormalization-point independent and its value can be compared with

$$\frac{-m\langle \bar{q}q \rangle_\pi}{f_\pi}\frac{1}{m_\sigma^2} = 3.6 \ \text{MeV}; \tag{79}$$

i.e., the magnitude of n_σ is typical of effects driven by dynamical chiral symmetry breaking. We can also define a $\sigma\bar{q}q$ coupling:

$$g_{\sigma\bar{q}q} := \Gamma_\sigma(0;Q)|_{Q^2=-m_\sigma^2} = 12.6, \tag{80}$$

whose magnitude can be placed in context via a comparison with $g_{\pi\bar{q}q} = 11.8$ obtained using the separable model's analog of the quark-level Goldberger-Treiman relation, Eq. (17).

To calculate the expectation value in Eq. (66) we use

$$\Gamma_m(k;Q) = m\Gamma_{\mathbf{1}}(k;Q) \tag{81}$$

as our impulse approximation probe in Eqs. (A28)–(A32) and obtain $\sigma(q^2) = s(q^2)$ by combining the contributions according to Eqs. (70),(A33). This yields the value of σ presented in Table I, with the relative strength of the contribution from the various diagrams listed in Table II.

The form factor is depicted in Fig. 5 where the evolution to the σ-meson pole is evident. Fitting ($t = -q^2$)

$$\sigma(t) = g_{\sigma NN}\frac{m n_\sigma}{1 - t/m_\sigma^2}, \quad t \in [0.1, 0.5] \ \text{GeV}^2, \tag{82}$$

which isolates the residue associated with $\Gamma_m(k;Q)$, we obtain the on-shell coupling: $g_{\sigma NN} = 27.3$. This coupling can also be calculated directly using the solution of the homogeneous Bethe-Salpeter equation and that yields

$$g_{\sigma NN} = 27.7, \tag{83}$$

in agreement within Monte Carlo errors. Equation (82) alone overestimates the magnitude of our calculated $\sigma(t)$ everywhere except in the neighborhood of the pole.

As the lowest-mass pole-solution of Eq. (71), our σ meson is distinct from the phenomenological meson introduced in potential models to mock-up two-pion exchange.[6] However, we can estimate a coupling relevant to meson exchange models by introducing $g_\sigma(t)$:

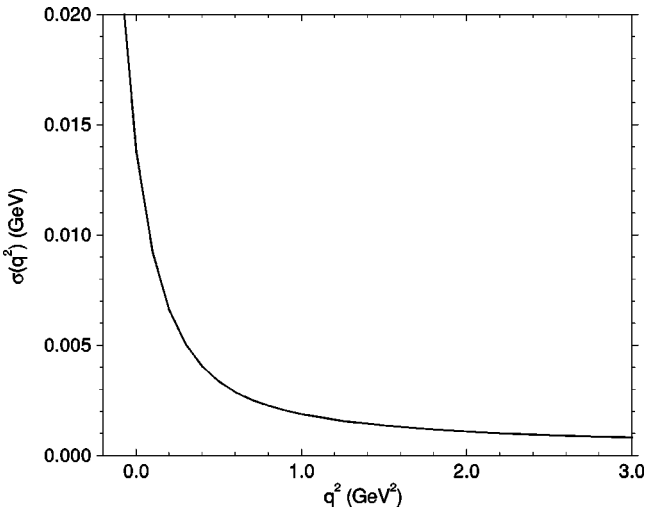

FIG. 5. Our calculated $\sigma(q^2)$. The rapid increase with decreasing q^2 is associated with the evolution to the σ-meson pole. On this scale, $\sigma(q^2)$ calculated without the $t_{2,3}(Q^2)$ contributions is indistinguishable from the full calculation.

$$\sigma(t) =: g_\sigma(t)\frac{m n_\sigma}{1 - t/m_\sigma^2}, \tag{84}$$

and a fit to our calculated $\sigma(t)$ yields

$$g_\sigma(t) = 1.61 + 2.61\frac{1}{(1 - t/\Lambda_\sigma^2)^{10}}, \quad \Lambda_\sigma = 1.56 \ \text{GeV}, \tag{85}$$

where the large exponent merely reflects the rapid evolution from bound state to continuum dominance of the vertex in the spacelike region. At the mock-σ mass: $m_\sigma^{2\pi} = 0.5$ GeV,

$$g_\sigma := g_\sigma((m_\sigma^{2\pi})^2) = 9.3, \tag{86}$$

which is listed in Table I and compared with a phenomenologically inferred value: $g_\sigma = 10$ [39]. We note that $g_\sigma(4m_\pi^2) = 5.2$ so that this comparison is meaningful on a relevant phenomenological domain. Further, $g_\sigma(q^2 \to \infty) = 1.61$ and we, therefore, find that $\sigma(q^2)$ is well approximated by a single monopole for $q^2 > 1$ GeV^2. However, the residue is very different from the on-shell value. The scalar radius of the nucleon is obtained from

[6]The separable model [13] realizes a rainbow-ladder truncation of the quark DSE and meson Bethe-Salpeter equation, which is likely inaccurate in the 0^{++} channel [37]. The defect is tied to the difficulties encountered in understanding the composition of scalar resonances below 1.4 GeV [38].

$$\langle r^2_{\sigma NN}\rangle := -\frac{6}{\sigma}\frac{d\sigma(q^2)}{dq^2}\bigg|_{q^2=0} \tag{87}$$

and our calculated result is listed in Table I, in comparison with an inferred value [39].

VII. SUMMARY AND CONCLUSION

In Ref. [8] we introduced a simple model of the nucleon's Fadde'ev amplitude that represents the nucleon as a bound state whose constituents are a confined dressed quark and confined dressed-scalar diquark, and fixed its parameters in a calculation of nucleon electromagnetic properties. Herein we employ that model in a study of a range of nucleon form factors that can be identified with those used extensively in phenomenological NN potentials and meson-exchange models. These calculations require knowledge of the relevant meson Bethe-Salpeter amplitudes and three-point vertex functions. However, they have been determined in the application of Dyson-Schwinger equation models to non-nucleonic processes. It is an important result that this simple model provides a uniformly good description of nucleon properties and, where there are discrepancies with experimental data, a cause and a means for its amelioration are readily identified. Our study demonstrates that it is realistic to hope for useful constraints on meson-exchange models from well-constrained models of hadron structure.

Our calculations suggest that the nucleon form factors are ''soft'' and there is no sign that this is a model-dependent result. The couplings generally agree well with those fitted in meson-exchange models. The only significant discrepancy is that we find $0.4 \lesssim f_{\omega NN}/g_{\omega NN} \lesssim 1.0$, whereas the conventional model assumption is $f_{\omega NN}=0$. Comparison with our calculation of the nucleon's isoscalar electromagnetic form factor, however, suggests that $f_{\omega NN}$ is the one coupling particularly sensitive to neglecting the axial-vector diquark. Hence a conclusive determination of $f_{\omega NN}$ must await its incorporation.

A primary requirement for improving our model is the inclusion of the axial-vector diquark correlation. In our study of g_A we saw that it can contribute up to $\sim 25\%$, and Fadde'ev equation studies show [10,34,35] that it provides a necessary $\sim 33\%$ reduction of the quark+scalar-diquark nucleon mass. Also important in our analysis of g_A was an elucidation of the role played by transverse parts of the dressed-quark-axial-vector vertex that are regular at $Q^2=0$. A simple model that allowed for the constrained leakage of the a_1-meson pole contribution into the spacelike region showed that terms unrestricted by the axial-vector Ward-Takahashi identity provide $\sim 20\%$ of the magnitude of g_A. This sensitivity of the result to such elements makes important a numerical solution of the axial-vector vertex equation, a calculation for which the study of the vector vertex [29] serves as an exemplar.

Our analysis of the nucleon σ term is particularly interesting because it illustrates the only method that allows an unambiguous off-shell extrapolation in the estimation of meson-nucleon form factors. An essential element in the impulse approximation calculation of the scalar form factor: $\sigma(q^2)$, is the dressed-quark-scalar vertex and we used a separable model to obtain it as the solution of the inhomogeneous scalar vertex equation. This solution exhibits a simple pole at $Q^2=-m_\sigma^2$ and hence so does $\sigma(q^2)$. The residue of that pole gives the σ-meson nucleon coupling. However, the inhomogeneous vertex equation admits a solution for arbitrary Q^2, which describes the Q^2-dependent dressed-quark-scalar coupling and hence allows a direct and consistent determination of $\sigma=\sigma(q^2=0)$. That Q^2-dependent coupling exemplifies the necessary elements in studies of those meson-nucleon form factors that truly represent correlated quark exchange. Our calculation of $\sigma(q^2)$ and the model (b) calculation of g_A are analogs of Ref. [29], which elucidates similar aspects of the electromagnetic pion form factor, making explicit the ρ-meson contribution and its leakage away from $Q^2=-m_\rho^2$.

As noted above, to proceed it is important to include axial-vector diquark correlations. Without them we cannot describe the Δ resonance, and the $N\to\Delta$ transition is an important probe of hadron structure and models; e.g., resonant quadrupole strength in this transition can be interpreted as a signal of nucleon deformation [40]. The existence of strong final-state interactions muddies this interpretation and means that nucleon structure models such as ours cannot be compared directly with data. However, they can be used as a foundation in the application of detailed reaction models [41] and thereby provide a connection between the nucleon's quark-gluon content, its ''shape'' and data.

ACKNOWLEDGMENTS

We acknowledge interactions with R. Alkofer, T.-S.H. Lee, H.B. O'Connell, and P.C. Tandy. This work was supported by the U.S. Department of Energy, Nuclear Physics Division, under Contract No. W-31-109-ENG-38, and benefited from the resources of the National Energy Research Scientific Computing Center. S.M.S. is grateful for financial support from the A.v. Humboldt Foundation.

APPENDIX: COLLECTED FORMULAS

1. Pion-nucleon

For the πNN coupling, Fig. 1 represents

$$\Lambda_\pi^{1j}(q,P) = 3\int \frac{d^4l}{(2\pi)^4}\psi(K,p_3+q)\Delta(K)\psi(K,p_3) \times \Lambda_\pi^{qj}(p_3+q,p_3), \tag{A1}$$

with $K=\frac{2}{3}P+l$, $p_3=\frac{1}{3}P-l$, $p_2=K/2-k$, $\Lambda_\pi^{qj}(k_1,k_2)=S(k_1)\Gamma_\pi^j(k_r;k_T)S(k_2)$, $k_r=\frac{1}{2}(k_1-k_2)$, $k_T=k_1+k_2$,

$$\Lambda_\pi^{2j}(q,P)=0; \tag{A2}$$

i.e., there is not a direct pion–scalar-diquark coupling because of parity conservation,

$$\Lambda_\pi^{3j}(q,P) = -6\int \frac{d^4k}{(2\pi)^4}\frac{d^4l}{(2\pi)^4}\Omega(p_1+q,p_3,p_2) \times\Omega(p_1,p_2,p_3)S(p_2)\Lambda_\pi^{qj}(p_1,p_1+q)S(p_3), \tag{A3}$$

$$\Lambda_\pi^{4j}(q,P) = 6\int \frac{d^4k}{(2\pi)^4}\frac{d^4l}{(2\pi)^4}\Omega(p_1,p_3,p_2+q) \times\Omega(p_1,p_2,p_3)\Lambda_\pi^{qj}(p_2+q,p_2)S(p_1)S(p_3), \tag{A4}$$

$$\Lambda_\pi^{5j}(q,P) = 6\int \frac{d^4k}{(2\pi)^4}\frac{d^4l}{(2\pi)^4}\Omega(p_1,p_3+q,p_2) \times\Omega(p_1,p_2,p_3)S(p_2)S(p_1)\Lambda_\pi^{qj}(p_3+q,p_3), \tag{A5}$$

with $6=\varepsilon_{c_1c_2c_3}\varepsilon_{c_1c_2c_3}$ and

$$\Omega(p_1,p_2,p_3) = \psi(p_1+p_2,p_3)\Delta(p_1+p_2)\Gamma(p_1,p_2). \tag{A6}$$

2. Vector-meson–nucleon

For the vector meson coupling, Fig. 1 represents

$$\Lambda_\mu^{1j}(q,P) = 3\int \frac{d^4l}{(2\pi)^4}\psi(K,p_3+q)\Delta(K)\psi(K,p_3) \times\Lambda_\mu^{qj}(p_3+q,p_3), \tag{A7}$$

$$\Lambda_\mu^{2j}(q,P) = 6\int \frac{d^4k}{(2\pi)^4}\frac{d^4l}{(2\pi)^4} \times\Omega(p_1+q,p_2,p_3)\Omega(p_1,p_2,p_3) \times\mathrm{tr}_{DF}[\Lambda_\mu^{qj}(p_1+q,p_1)S(p_2)]S(p_3), \tag{A8}$$

$$\Lambda_\mu^{3j}(q,P) = (-1)^I 6\int \frac{d^4k}{(2\pi)^4}\frac{d^4l}{(2\pi)^4}\Omega(p_1+q,p_3,p_2) \times\Omega(p_1,p_2,p_3)S(p_2)\Lambda_\mu^{qj}(p_1,p_1+q)S(p_3), \tag{A9}$$

$$\Lambda_\mu^{4j}(q,P) = 6\int \frac{d^4k}{(2\pi)^4}\frac{d^4l}{(2\pi)^4} \times\Omega(p_1,p_3,p_2+q)\Omega(p_1,p_2,p_3) \times\Lambda_\mu^{qj}(p_2+q,p_2)S(p_1)S(p_3), \tag{A10}$$

$$\Lambda_\mu^{5j}(q,P) = 6\int \frac{d^4k}{(2\pi)^4}\frac{d^4l}{(2\pi)^4}\Omega(p_1,p_3+q,p_2) \times\Omega(p_1,p_2,p_3)S(p_2)S(p_1) \times\Lambda_\mu^{qj}(p_3+q,p_3), \tag{A11}$$

with $\Lambda_\mu^{qj}(k_1,k_2)=S(k_1)\Gamma_\mu^j(k_r;k_T)S(k_2)$ and $\Gamma_\mu^j(k_r;k_T)$ the Bethe-Salpeter-like amplitude of Eq. (37) whose normalization is determined by

$$2\mathcal{N}_V^2\delta^{\alpha\beta}Q_\mu = \tfrac{1}{3}\,\mathrm{tr}_{\mathrm{CDF}}\int\frac{d^4k}{(2\pi)^4}\Big[\Gamma_\nu^\alpha(k;-Q)\frac{\partial S(k_+)}{\partial Q_\mu}\Gamma_\nu^\beta(k;Q)S(k_-) + \Gamma_\nu^\alpha(k;-Q)S(k_+)\Gamma_\nu^\beta(k;Q)\frac{\partial S(k_-)}{\partial Q_\mu}\Big]_{Q^2=-M_V^2}, \tag{A12}$$

where $k_\pm = k\pm Q/2$. The flavor trace ensures that Λ_μ^{2j} contributes only to the isoscalar coupling. This merely reflects the fact that in an isospin symmetric theory there cannot be a three-point iso-vector-scalar-scalar vertex. Further, Λ_μ^{3j} contributes with opposite signs to the $\omega^{(I=0)}$ and $\rho^{(I=1)}$ couplings. The complete vertex is

$$\Lambda_\mu^j(q,P) = \Lambda_\mu^{1j}(q,P) + 2\sum_{n=2}^{5}\Lambda_\mu^{nj}(q,P). \tag{A13}$$

3. Axial-vector–nucleon

Model (b) for the dressed-quark-axial-vector vertex involves the Bethe-Salpeter amplitude for the a_1 meson, which in the separable model of Ref. [13] has the form (terms quadratic in k are suppressed in this model)

$$\Gamma_\mu^{a_1}(\overline{k},\hat{Q}) = i\vec{\tau}[\gamma_5\gamma_\mu^T e_1^{a_1}\overline{G}(x) + e_2^{a_1}\epsilon_{\lambda\mu\nu\sigma}\gamma_\lambda\overline{k}_\nu\hat{Q}_\sigma\overline{F}(x)], \tag{A14}$$

where $\overline{k}=k/\lambda$, $\lambda=0.566$ GeV is the model's mass scale, $\hat{Q}_\mu = Q_\mu/|Q^2|^{1/2}$, $\gamma_\mu^T=(\gamma_\mu - Q_\mu\gamma\cdot Q/Q^2)$ and

$$\overline{F}(x) = \frac{1}{a}[\overline{A}(x)-1], \quad \overline{G}(x) = \frac{1}{b}[\overline{B}(x)-\overline{m}], \tag{A15}$$

with calculated constants

$$\overline{a}=(0.359)^2, \quad \overline{b}=(0.296)^2. \tag{A16}$$

Herein [30] $\overline{A}(x)$, $\overline{B}(x)$ are modified dressed-quark propagator functions obtained in the usual way from

$$\overline{\sigma}_S^{a_1}(x) = 2\hat{m}\mathcal{F}(2(x+\hat{m}^2)) + \mathcal{F}(b_1x)\mathcal{F}(b_3x)\mathcal{F}((\epsilon_S x)^2) \times[b_0+b_2^{a_1}\mathcal{F}(\epsilon x)], \tag{A17}$$

$$\overline{\sigma}_V^{a_1}(x)=\frac{2(x+\hat{m}^2)-e^{-\epsilon_V^2(x+\hat{m}^2)^2}+e^{-2(x+\hat{m}^2)}}{2(x+\hat{m}^2)^2}, \tag{A18}$$

where

$$\hat{m}=0.0081, \quad b_2^{a_1}=0.863, \quad \epsilon_S=0.482, \quad \epsilon_V=0.1, \tag{A19}$$

and the other parameters are given in Eq. (12).

The separable model yields m_{a_1} in Eq. (A21) and the eigenvector

$$e_1^{a_1}=0.145, \quad e_2^{a_1}=1.69, \tag{A20}$$

which is canonically normalized using Eq. (A12) evaluated with Eqs. (A14)–(A19). This Bethe-Salpeter amplitude yields f_{a_1} in Eq. (A21).

	m_{a_1} (GeV)	f_{a_1} (GeV)
Calc.	1.34	0.221
Obs.	1.23±0.040 [21]	0.203±0.018 [31]

(A21)

NB: This model predicts that the $\gamma_5\gamma_\mu$ term is subdominant in the a_1 meson. The dominant $e_2^{a_1}$ term characterizes constituents with relative orbital motion.

For the axial-vector coupling, Fig. 1 represents

$$\Lambda_{5\mu}^{1j}(q,P)=3\int\frac{d^4l}{(2\pi)^4}\,\psi(K,p_3+q)\Delta(K)\psi(K,p_3)\times\Lambda_{5\mu}^{qj}(p_3+q,p_3), \tag{A22}$$

$$\Lambda_{5\mu}^{2j}(q,P)=0, \tag{A23}$$

$$\Lambda_{5\mu}^{3j}(q,P)=6\int\frac{d^4k}{(2\pi)^4}\frac{d^4l}{(2\pi)^4}\Omega(p_1+q,p_3,p_2)\times\Omega(p_1,p_2,p_3)S(p_2)\Lambda_{5\mu}^{qj}(p_1,p_1+q)S(p_3), \tag{A24}$$

$$\Lambda_{5\mu}^{4j}(q,P)=6\int\frac{d^4k}{(2\pi)^4}\frac{d^4l}{(2\pi)^4}\Omega(p_1,p_3,p_2+q)\times\Omega(p_1,p_2,p_3)\Lambda_{5\mu}^{qj}(p_2+q,p_2)S(p_1)S(p_3), \tag{A25}$$

$$\Lambda_{5\mu}^{5j}(q,P)=6\int\frac{d^4k}{(2\pi)^4}\frac{d^4l}{(2\pi)^4}\Omega(p_1,p_3+q,p_2)\times\Omega(p_1,p_2,p_3)S(p_2)S(p_1)\Lambda_{5\mu}^{qj}(p_3+q,p_3), \tag{A26}$$

$\Lambda_{5\mu}^{qj}(k_1,k_2)=S(k_1)\Gamma_{5\mu}^j(k_r;k_T)S(k_2)$ with $\Gamma_{5\mu}^j(k_r;k_T)=\Gamma_{5\mu}^{Rj}(k_r;k_T)$, the regular part of the dressed-axial-vector-quark vertex defined by model (a), Eqs. (57),(60); or model (b), Eqs. (57),(61). Λ_μ^{2j} vanishes for the same reason that Λ_π^{2j} does and the complete vertex is

$$\Lambda_{5\mu}^{j}(q,P)=\Lambda_{5\mu}^{1j}(q,P)+2\sum_{n=2}^{5}\Lambda_{5\mu}^{nj}(q,P). \tag{A27}$$

4. σ term

The contributions to the scalar-nucleon vertex are

$$\Lambda_{\mathbf{1}}^{1}(q,P)=3\int\frac{d^4l}{(2\pi)^4}\,\psi(K,p_3+q)\Delta(K)\psi(K,p_3)\times\Lambda_m^q(p_3+q,p_3), \tag{A28}$$

$$\Lambda_{\mathbf{1}}^{2}(q,P)=12\int\frac{d^4k}{(2\pi)^4}\frac{d^4l}{(2\pi)^4}\times\Omega(p_1+q,p_2,p_3)\Omega(p_1,p_2,p_3)\times\mathrm{tr}_D[\Lambda_m^q(p_1+q,p_1)S(p_2)]S(p_3), \tag{A29}$$

$$\Lambda_{\mathbf{1}}^{3}(q,P)=6\int\frac{d^4k}{(2\pi)^4}\frac{d^4l}{(2\pi)^4}\times\Omega(p_1+q,p_3,p_2)\Omega(p_1,p_2,p_3)S(p_2)\times\Lambda_m^q(p_1,p_1+q)S(p_3), \tag{A30}$$

$$\Lambda_{\mathbf{1}}^{4}(q,P)=6\int\frac{d^4k}{(2\pi)^4}\frac{d^4l}{(2\pi)^4}\Omega(p_1,p_3,p_2+q)\times\Omega(p_1,p_2,p_3)\Lambda_m^q(p_2+q,p_2)S(p_1)S(p_3), \tag{A31}$$

$$\Lambda_{\mathbf{1}}^{5}(q,P)=6\int\frac{d^4k}{(2\pi)^4}\frac{d^4l}{(2\pi)^4}\Omega(p_1,p_3+q,p_2)\times\Omega(p_1,p_2,p_3)S(p_2)S(p_1)\Lambda_m^q(p_3+q,p_3), \tag{A32}$$

with $\Lambda_m^q(k_1,k_2)=S(k_1)\Gamma_m(k_r;k_T)S(k_2)$, and

$$\Lambda_{\mathbf{1}}(q,P)=\Lambda_{\mathbf{1}}^{1}(q,P)+2\sum_{n=2}^{5}\Lambda_{\mathbf{1}}^{n}(q,P). \tag{A33}$$

[1] R. Machleidt, Adv. Nucl. Phys. **19**, 189 (1989).
[2] R.B. Wiringa, V.G. Stoks, and R. Schiavilla, Phys. Rev. C **51**, 38 (1995).
[3] T. Sato and T.S. Lee, Phys. Rev. C **54**, 2660 (1996).
[4] R. Abegg *et al.*, Phys. Rev. C **57**, 2126 (1998), and references therein.
[5] C.J. Burden, J. Praschifka, and C.D. Roberts, Phys. Rev. D **46**, 2695 (1992); H.B. O'Connell, B.C. Pearce, A.W. Thomas, and A.G. Williams, Phys. Lett. B **336**, 1 (1994).
[6] P.C. Tandy, in *Future Directions in Quark Nuclear Physics*, edited by A.W. Thomas and A.G. Williams (World Scientific, Singapore, 1997), pp. 62–71.
[7] P.C. Tandy, Fiz. B **8**, 295 (1999).
[8] J.C.R. Bloch, C.D. Roberts, S.M. Schmidt, A. Bender, and M.R. Frank, Phys. Rev. C **60**, 062201 (1999).
[9] R.T. Cahill, C.D. Roberts, and J. Praschifka, Aust. J. Phys. **42**, 129 (1989); C.J. Burden, R.T. Cahill, and J. Praschifka, *ibid.* **42**, 147 (1989).
[10] N. Ishii, W. Bentz, and K. Yazaki, Nucl. Phys. **A587**, 617 (1995).
[11] M. Oettel, G. Hellstern, R. Alkofer, and H. Reinhardt, Phys. Rev. C **58**, 2459 (1998).
[12] Jefferson Lab Hall A Collaboration, M.K. Jones *et al.*, Phys. Rev. Lett. **84**, 1398 (2000).
[13] C.J. Burden, L. Qian, C.D. Roberts, P.C. Tandy, and M.J. Thomson, Phys. Rev. C **55**, 2649 (1997).
[14] C.D. Roberts and A.G. Williams, Prog. Part. Nucl. Phys. **33**, 477 (1994).
[15] C.J. Burden, C.D. Roberts, and M.J. Thomson, Phys. Lett. B **371**, 163 (1996).
[16] C.D. Roberts, Fiz. Élem. Chastits At. Yadra **30**, 537 (1999) [Phys. Part. Nuclei **30**, 223 (1999)].
[17] P. Maris, C.D. Roberts, and P.C. Tandy, Phys. Lett. B **420**, 267 (1998).
[18] P. Maris and C.D. Roberts, Phys. Rev. C **58**, 3659 (1998).
[19] F.T. Hawes and M.A. Pichowsky, Phys. Rev. C **59**, 1743 (1999).
[20] M.A. Ivanov, Y.L. Kalinovsky, and C.D. Roberts, Phys. Rev. D **60**, 034018 (1999).
[21] Particle Data Group, C. Caso, *et al.*, Eur. Phys. J. C **3**, 1 (1998).
[22] P. Maris and C.D. Roberts, Phys. Rev. C **56**, 3369 (1997).
[23] L.C. Hollenberg, C.D. Roberts, and B.H. McKellar, Phys. Rev. C **46**, 2057 (1992); R. Alkofer, A. Bender, and C.D. Roberts, Int. J. Mod. Phys. A **10**, 3319 (1995); M.A. Pichowsky, S. Walawalkar, and S. Capstick, Phys. Rev. D **60**, 054030 (1999).
[24] K.L. Miller *et al.*, Phys. Rev. D **26**, 537 (1982); T. Kitagaki *et al.*, *ibid.* **28**, 436 (1983).
[25] SESAM Collaboration, S. Gusken *et al.*, Phys. Rev. D **59**, 054504 (1999).
[26] P.C. Tandy, in *Quantum Chromodynamics*, edited by H.M. Fried and B. Müller (World Scientific, Singapore, 1997), pp. 162–170; P.C. Tandy, L. Qian, and S. Banerjee, Nucl. Phys. **A631**, 482c (1998).
[27] A.W. Thomas and K. Holinde, Phys. Rev. Lett. **63**, 2025 (1989).
[28] P. Maris and P.C. Tandy, Phys. Rev. C **60**, 055214 (1999).
[29] P. Maris and P.C. Tandy, Phys. Rev. C **61**, 045202 (2000).
[30] J.C.R. Bloch, Y.L. Kalinovsky, C.D. Roberts, and S.M. Schmidt, Phys. Rev. D **60**, 111502 (1999).
[31] N. Isgur, C. Morningstar, and C. Reader, Phys. Rev. D **39**, 1357 (1989).
[32] G. Hellstern, R. Alkofer, M. Oettel, and H. Reinhardt, Nucl. Phys. **A627**, 679 (1997).
[33] R. Alkofer (unpublished).
[34] Reference [11] cf. Ref. [32].
[35] R.T. Cahill and S.M. Gunner, Fiz. B **7**, 171 (1998).
[36] C.J. Burden and M.A. Pichowsky (unpublished).
[37] C.D. Roberts, in *Quark Confinement and the Hadron Spectrum II*, edited by N. Brambilla and G.M. Prosperi (World Scientific, Singapore, 1997), pp. 224–230.
[38] M. Boglione and M.R. Pennington, Eur. Phys. J. C **9**, 11 (1999).
[39] B. Friman and M. Soyeur, Nucl. Phys. **A600**, 477 (1996).
[40] C. Mertz *et al.*, nucl-ex/9902012.
[41] T. Yoshimoto, T. Sato, M. Arima, and T.S. Lee, Phys. Rev. C **61**, 065203 (2000), this issue.